Experimental Study on the Ultraprecision Ductile Machinability of Single-Crystal Germanium*

Jiwang YAN**, Kouki MAEKAWA**,
Jun'ichi TAMAKI** and Akihiko KUBO**

Single-crystal germanium is an important infrared optical material. In the present work, single-point diamond turning experiments on single-crystal germanium (100), (110) and (111) planes were conducted in order to examine their ultraprecision machining characteristics. Three kinds of surface textures and chip morphologies were observed during the brittle-ductile transition of the machining mode. The brittle-ductile boundary changed significantly with the crystal orientations of the workpieces. Due to the crystallographic anisotropy, micro-fractures were generated on the workpiece surface in a radial pattern from the rotation center. However, it was possible to produce completely ductile-cut surfaces on all crystal orientations by using undeformed chip thicknesses smaller than a critical value, namely, the minimum critical undeformed chip thickness, which was approximately 60 nm under the present conditions. Compared to wet cutting, dry cutting was beneficial for ductile machining on a few specific crystal orientations. The findings in this study provide criterions for determining process parameters for the fabrication of aspherical and diffraction infrared optics using single-crystal germanium.

Key Words: Cutting, Ultraprecision Machining, Machinability, Diamond Turning, Ductile Regime Machining, Germanium, Single Crystal, Brittle Ductile Transition, Optical Component

1. Introduction

Single-crystal germanium (Ge) is not only a semiconductor substrate material for the fabrication of micro electro mechanical system (MEMS) components, but also an important infrared optical material. It has very high permeability and high refractive index in the infrared range from 2 to 14 μm wavelength. Thus, it is an excellent substrate material for infrared optical lenses with extensive applications in thermal imaging systems, dark-field optical instruments, infrared astronomical telescopes, and so on. Recently, the demands for complex-shape infrared optical components, such as aspherical lenses, Fresnel lenses and diffraction grating lenses, are increasing remarkably. On the other hand, germanium is nominally a hard brittle material, having very low fracture toughness and relatively high hardness. Due to this nature, germanium is very difficult to machine. Conventionally, it has to be finished by mechanical or chemomechanical polishing for an optical surface. However, the polishing processes are not suitable for fabricating complicated shapes such as aspherical surfaces and diffraction surfaces which have discontinuously curved profiles.

An alternative machining technology is single-point diamond turning (SPDT). SPDT has been known to be capable of machining optical components with complex geometries through extremely precise numerical control of the tool path and the microscopic machining behavior. Conventionally, SPDT has been

* Received 18 September, 2003 (No. 03-4114)
** Department of Mechanical Engineering, Kitami Institute of Technology, 165 Koen-cho, Kitami, Hokkaido 090-8507, Japan. E-mail: yanjw@mail.kitami-it.ac.jp

used to machine ductile nonferrous metal materials. In the recent decade, a few hard brittle materials including germanium have also been demonstrated to be machinable by SPDT[1),2)]. Previous studies have also revealed that the plastic deformation of germanium during the indentation, scratching and machining tests originates from the high-pressure phase transformation[3),4)]. These findings provided insights into the fundamental physics governing the machining mechanism and contributed significantly to the ductile regime machining technology. However, to date, there is no available literature on the quantitative criterions for determining process parameters for the fabrication of precise optics from germanium. In particular, because germanium is a crystalline material with strong crystallographic anisotropy, the microscopic mechanical properties vary with crystal orientations, resulting in significantly different processing behaviors. The crystallographic effect will cause nonuniformity in surface quality and eventually limit the productivity of the ductile machining process.

In the present work, we conducted submicrometer-nanometer level SPDT experiments on single-crystal germanium substrates with different crystal orientations in an attempt to examine their ductile machinability for fabricating high-quality aspherical and diffraction optics. The effects of the crystal orientations on the machining mechanisms were emphatically investigated.

2. Experimental Procedures

2.1 Ultraprecision machining apparatus

The experiments were carried out on a three-axis numerically controlled ultraprecision diamond lathe, NACHI-ASP15. Figure 1 is a photograph of the main section of the machine. The machine has an ultraprecision air-bearing spindle, two perpendicular linear tables (X- and Z-axes) and a rotary table (B-axis). The linear tables are supported by high-stiffness hydrostatic bearings and are driven by servomotors via hydrostatic screws, allowing smooth nanometric movement with negligible mechanical friction. The rotary table is also supported by hydrostatic bearings and driven by a friction drive in order to prevent from non-driven backlash movements. Laser hologram scales are used to accurately position all these tables. Under precise numerical control, the linear tables can be moved at 10 nm per step and the rotary table can be rotated with an angular resolution of 0.001°. To isolate the machine from environmental vibration, the main section of the machine was fixed to a granite bed, which is supported by a set of air mounts.

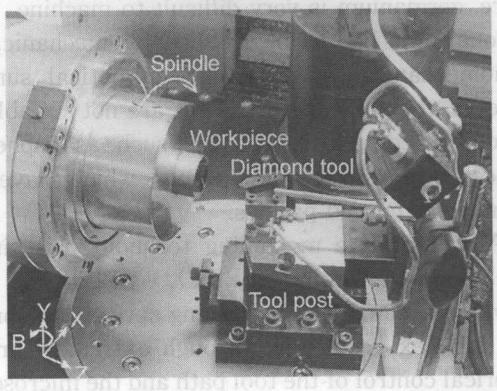

Fig. 1 Photograph of the experimental apparatus

2.2 Diamond tools

A straight-nosed cutting tool[5] made of single-crystal diamond was used for machining. The machining model is schematically shown in Fig. 2. The tool cuts longitudinally with periodical transverse feeds hence regular micro grooves can be produced on the workpiece surface. For this tool geometry, undeformed chip thickness (h) is uniform across the entire width of the cutting edge. Thus, the relationships between the surface texture and the undeformed chip thickness are unambiguous and readily studied. The relationship among the undeformed chip thickness h, the cutting edge angle κ and the tool feed f can be described by Eq.(1):

$$h = f \cdot \sin \kappa \qquad (1)$$

By using a sufficiently small cutting edge angle κ and/or a small tool feed f, it is possible to thin the undeformed chip thickness h to the nanometric range over the entire cutting region. This tool geometry has been used by one of the authors to fabricate large-diameter aspheric lenses of single-crystal silicon[6]. In the present experiments, a diamond tool having a 1.2 mm cutting edge, a −20° rake angle and a 26° relief angle was used. Using the −20° rake angle was to achieve both high ductile machinability and low cutting forces when cutting hard brittle materials[7]. The tool edge was examined by an atomic force microscope (AFM) and the edge radius was estimated to be ~50 nm. The cutting edge angle of the diamond tool was adjusted using the B-axis rotary table.

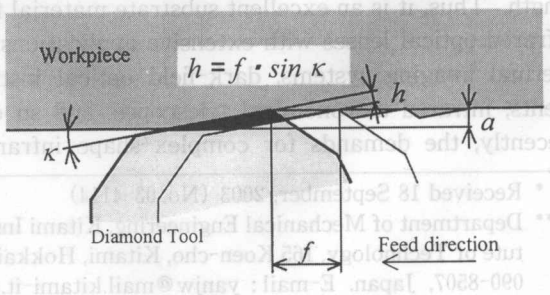

Fig. 2 Schematic of the machining model

Table 1 Experimental conditions

Tool material	Single-crystal diamond
Tool shape	Straight-nosed tool
Rake angle	−20°
Relief angle	26°
Work material	Single-crystal germanium (Ge)
Crystal plane	(111), (110), (100)
Depth of cut a	5 μm
Feed rate f	2.86 ~ 28.6 μm
Cutting edge angle κ	1°
Undeformed chip thickness h	50, 100, 200, 500 nm
Cutting speed	0 ~ 94 m/min
Cutting environment	Dry, kerosene mist

2.3 Work material

Single-crystal germanium substrates with (100), (110) and (111) surfaces were used as workpieces. These substrates are optical-grade pure germanium with no doping. The Mohs hardness of germanium is 6.3, which is between the hardness of silicon (7) and that of most glasses (5 - 5.5). The workpieces are 30 mm in diameter, 15 mm in thickness and obtained with ground finishes. The workpieces were bonded on diamond-turned aluminum blanks using a heat-softened glue and then vacuum-chucked to the machine spindle. For removing the damaged layer, precuts were performed with other diamond tools, providing mirror-like surfaces for experiments.

2.4 Machining conditions

Machining conditions used in the experiments are summarized in Table 1. Depth of cut a was set to 5 μm and cutting edge angle κ was set to 1°. Undeformed chip thickness h was set to four levels: 500, 200, 100 and 50 nm, by changing tool feed f in the range of 2.86 - 28.6 μm. The rotation rate of the machine spindle was fixed to 1 000 rpm, consequently, the cutting speed changes in the range of 0 - 94.2 m/min during facing cuts. Dry cuts and wet cuts using kerosene mist as coolant were performed respectively. A Nomarski differential interference microscope, a scanning electron microscope (SEM) and a laser probe scanning three-dimensional measuring machine, Mitaka NH-3SP, were used to examine and measure the machined surfaces. The cutting chips were observed using the SEM.

3. Results and Discussion

3.1 Machining regimes

Germanium is a highly brittle material. At room temperature, dislocations are difficult to move; hence, germanium responds in a brittle manner. In order to investigate the brittle-ductile transition behavior during the machining process, both the cutting chips and the machined surfaces were examined at various undeformed chip thicknesses.

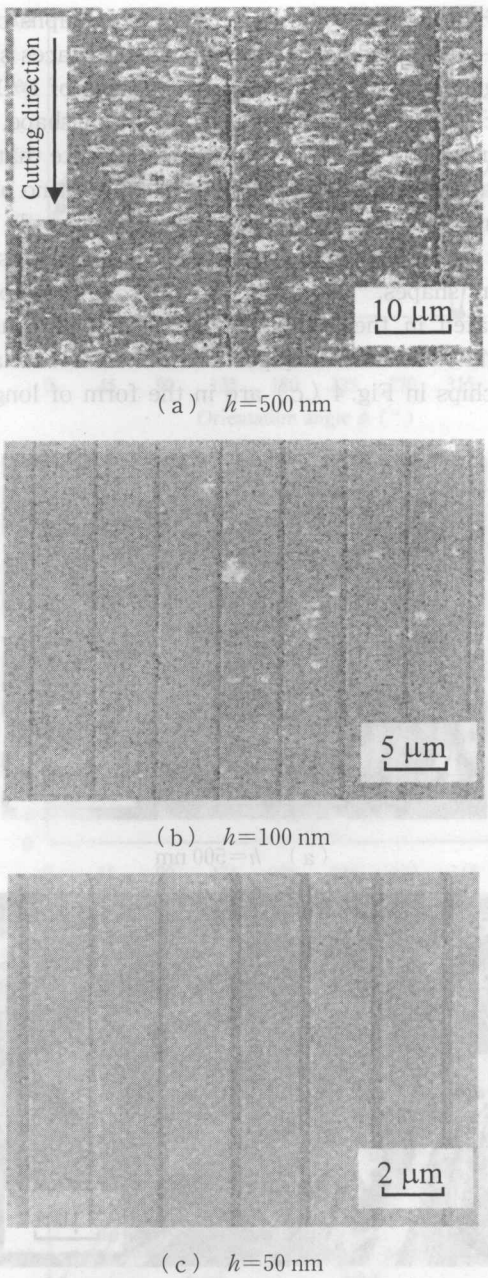

(a) h=500 nm

(b) h=100 nm

(c) h=50 nm

Fig. 3 SEM photographs of the cut surfaces at various undeformed chip thicknesses

Figure 3 (a)-(c) is SEM micrographs of the Ge (111) plane machined at undeformed chip thicknesses of 500, 100 and 50 nm, respectively. The micrographs were taken on the <110> orientation of the workpieces. In Fig. 3 (a), the surface is severely damaged with numerous micro craters and cracks, the size of which ranges in the order of 1 to 10 μm. In Fig. 3 (b), the surface is generally smooth, but dotted with a few micro-fractures in the order of 1 μm. In Fig. 3 (c), the surface is extremely smooth, without any micro-fractures. The parallel lines seen on the surfaces are the tool marks corresponding to the periodical tool feeds.

Figure 4 (a) - (c) is SEM micrographs of the chips corresponding to the machined surfaces shown in Fig. 3. The chips in Fig. 4 (a) consist of 1 - 10 μm particles and micro blocks, irregular in shape, with fractured appearance. These chips indicate that brittle fracture is predominant whereas almost no plastic deformation occurs during material removal. The chips in Fig. 4 (b) consist of needles and sticks with similar shapes. This kind of chips is akin to that generated in the machining of hard metals and is thought to be formed by periodical shear deformation. The chips in Fig. 4 (c) are in the form of long and continuous ribbons similar to those of ductile metal cutting. It is evident that plastic deformation occurred dominantly and no fracture took place in this machining regime.

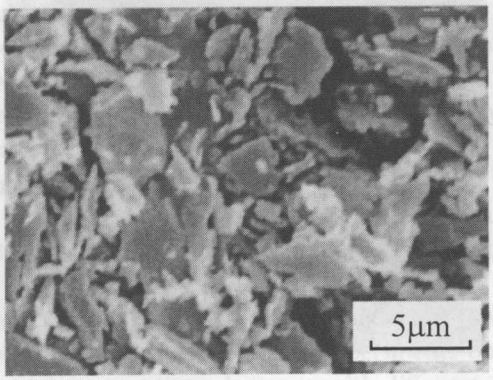

(a) h=500 nm

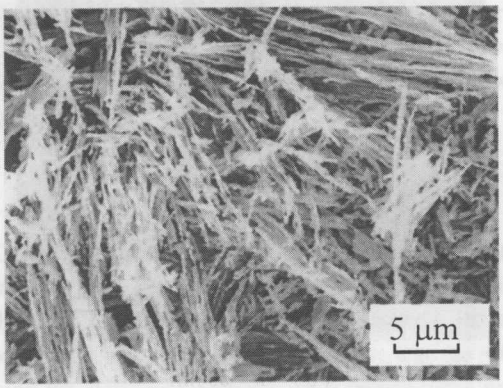

(b) h=100 nm

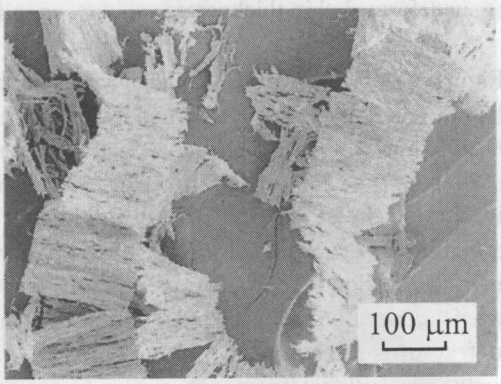

(c) h=50 nm

Fig. 4 SEM photographs of the chips at various undeformed chip thicknesses

The brittle-ductile transition in above machining process is considered to originate from the stress state transition in the cutting region. When undeformed chip thickness is large, there exists a concentration region of tensile stress near the cutting edge, whereas most of the upper region is under a low-stress state[8]. Due to the low fracture toughness of germanium, cracks will be immediately initiated in the tensile stress concentration region as the tool advances before any plastic deformation occurs. As the undeformed chip thickness is decreased, the scale of the low-stress region decreases. Moreover, since a commonly available diamond tool usually has an edge radius of a few tens of nanometers or larger, an extremely small undeformed chip thickness approaches the same order of the edge radius. The effective rake angle induced by the edge radius becomes a higher negative one than the nominal tool rake angle. Thus, the material in front of the cutting edge is downward suppressed and the compressive stress component becomes predominant[8]. This situation provides a stress state similar to the hydrostatic stress state under sharp indenters in an indentation test[9]. Immediately below the indenter, the material forms a radially expanding core, exerting a uniform hydrostatic pressure on its surroundings.

As known from the theory of plasticity, the magnitude of hydrostatic stress determines the extent of plastic deformation prior to fracture[10]. In other words, hydrostatic pressure determines strain at fracture, which in turn determines material ductility or brittleness. Bridgman proved that various nominally brittle materials are capable of ductile behavior under high external hydrostatic pressure[11]. Therefore, with sufficient hydrostatic pressure, plastic deformation will become preferable to crack generation even at a low temperature, and ductile regime material removal can be achieved. The hydrostatic pressure under the indenters in indentation tests is sufficiently high (~16 GPa) to make brittle materials such as silicon and germanium undergo plastic deformation[1]. It was also pointed out that a diamond-cubic to metallic phase transformation occurs under hardness indenters and in other situations where high hydrostatic pressure exists, which facilitate silicon and germanium to undergo plastic deformation[2]. In the same way, high hydrostatic pressure will also be generated in ultraprecision machining and facilitate the ductile regime material removal[12],[13].

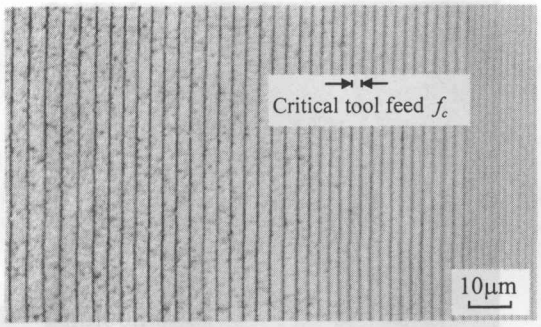

Fig. 5 Measurement of the critical tool feed for brittle-ductile transition

3.2 Brittle-ductile transition boundary

In order to determine process parameters for fabricating optical components by ductile regime machining, it is important to know quantitatively the critical undeformed chip thickness (d_c) at which the brittle-ductile transition occurs. The measurement of d_c can be accomplished by performing facing cuts at gradually varied tool feed while keeping the cutting edge angle constant. In this paper, the tool feed f was changed by 2 μm per step at a cutting edge angle of 1°, thus, the undeformed chip thickness h was changed by 30 nm per step. In this way, the brittle-ductile transition boundary can be measured. An example of the Nomarski micrograph of the surface machined under such conditions is shown in Fig. 5. As the tool feed decreases from the left to the right, the cutting mode transits from brittle to ductile. Micro-fractures begin to disappear at a critical tool feed f_c. The value of the critical undeformed chip thickness d_c is then calculated from f_c by Eq.(1). In Fig. 5, f_c=3.5 μm, thus d_c =60 nm.

3.3 Crystal orientation effects

Measurements of d_c were performed on different circumferential orientations of the workpieces. Figure 6 (a) - (c) shows the plots of critical undeformed chip thicknesses d_c versus the orientation angle of Ge (100), (110) and (111), respectively, under dry and wet conditions. The orientation angle is the angular deviation of the measurement point from the orientation flat (OF) that corresponds to <110>. In all the figures, periodical variations of d_c are observed during per revolution of the workpieces. In Fig. 6 (a), there are 8 peaks, 4 deep valleys and 4 shallow valleys. The maximum value of d_c ($d_{c\max}$) was 270 nm, and the minimum value ($d_{c\min}$) was 60 nm. Orientations corresponding to $d_{c\min}$ are 45, 135, 225, and 315°. These orientations are the most difficult to be ductile-machined for the Ge (100) plane. In Fig. 6 (b), d_c fluctuates more significantly than that in Fig. 6 (a). The $d_{c\max}$ was 450 nm, while the $d_{c\min}$ was only 60 nm. Orientations corresponding to $d_{c\min}$ are 60, 120, 240,

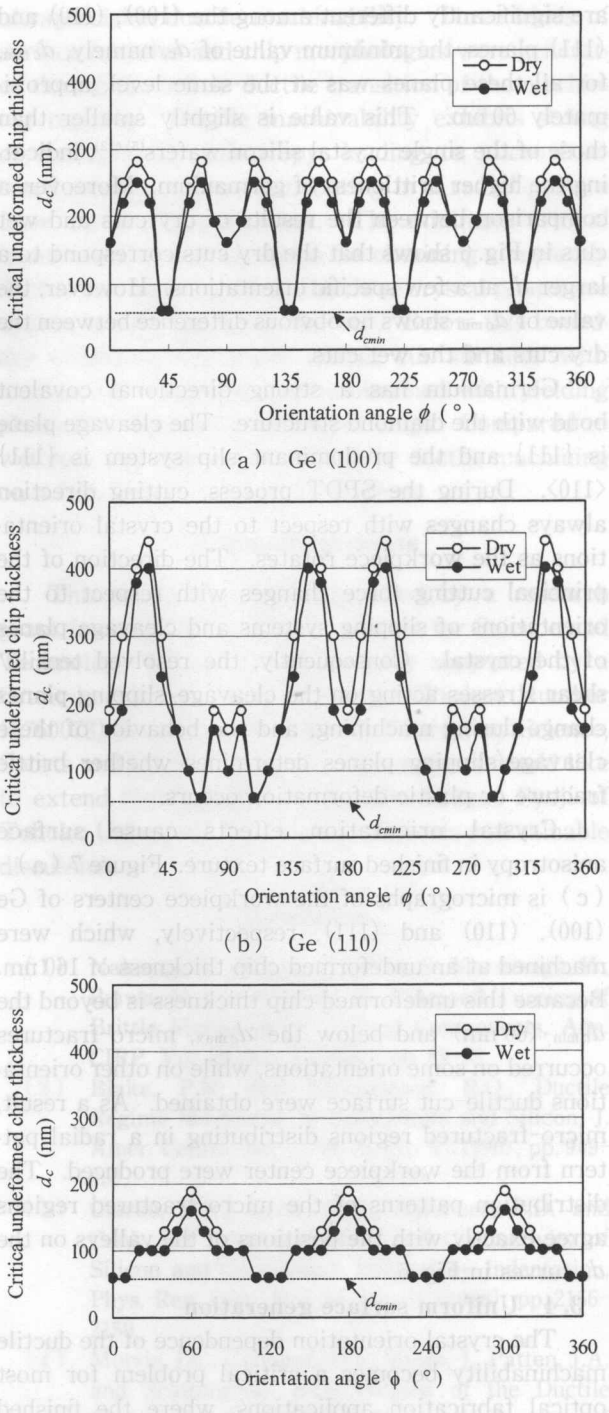

Fig. 6 Variations of the critical undeformed chip thickness with crystal orientation angle

and 300°. In Fig. 6 (c), the variation amplitude of d_c is smaller than that in Fig. 6 (a) and (b). Three valleys appeared at 0, 120 and 240°, corresponding to the $d_{c\min}$ of 60 nm.

These results illustrate that the brittle-ductile transition boundary varies significantly with the crystal orientation angle. On the other hand, despite that the variation patterns of d_c versus orientation angles

are significantly different among the (100), (110) and (111) planes, the minimum value of d_c, namely, $d_{c\,min}$, for all these planes was at the same level, approximately 60 nm. This value is slightly smaller than those of the single-crystal silicon wafers[5],[12], indicating the higher brittleness of germanium. Moreover, a comparison between the results of dry cuts and wet cuts in Fig. 6 shows that the dry cuts correspond to a larger d_c at a few specific orientations. However, the value of $d_{c\,min}$ shows no obvious difference between the dry cuts and the wet cuts.

Germanium has a strong directional covalent bond with the diamond structure. The cleavage plane is {111} and the predominant slip system is {111}〈110〉. During the SPDT process, cutting direction always changes with respect to the crystal orientations as the workpiece rotates. The direction of the principal cutting force changes with respect to the orientations of slipping systems and cleavage planes of the crystal. Consequently, the resolved tensile/shear stresses acting on the cleavage/slipping planes change during machining, and the behavior of these cleavage/slipping planes determines whether brittle fracture or plastic deformation occurs.

Crystal orientation effects cause surface anisotropy in finished surface texture. Figure 7 (a) - (c) is micrographs of the workpiece centers of Ge (100), (110) and (111), respectively, which were machined at an undeformed chip thickness of 160 nm. Because this undeformed chip thickness is beyond the $d_{c\,min}$ (60 nm) and below the $d_{c\,max}$, micro-fractures occurred on some orientations, while on other orientations ductile-cut surface were obtained. As a result, micro-fractured regions distributing in a radial pattern from the workpiece center were produced. The distribution patterns of the micro-fractured regions agree exactly with the positions of the valleys on the d_c curves in Fig. 6.

3.4 Uniform surface generation

The crystal orientation dependence of the ductile machinability becomes a critical problem for most optical fabrication applications, where the finished surface must be uniformly smooth and completely damage-free. These requirements, however, can be satisfied by using an undeformed chip thickness below the minimum critical undeformed chip thickness $d_{c\,min}$. Such an extremely small undeformed chip thickness can be immediately achieved by adopting a sufficiently small cutting edge angle $\varkappa$ and/or a small tool feed f, as shown in Fig. 2.

As a test cut, a Ge (111) workpiece was machined under the conditions: $\varkappa=1°$, $f=3.2\,\mu m$ and $a=5\,\mu m$. These conditions determine an undeformed chip thickness of 55 nm, which approaches the highest material

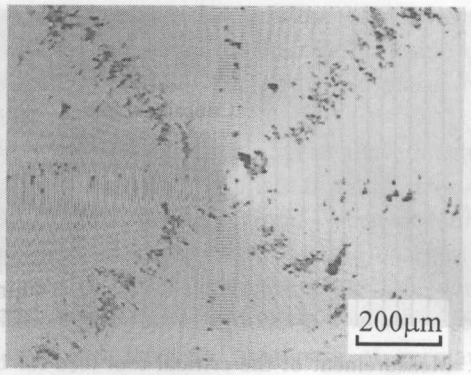

(a) Ge (100)

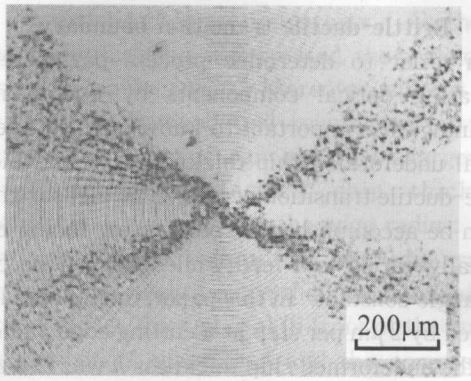

(b) Ge (110)

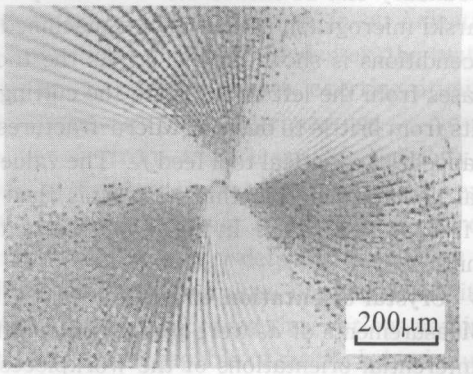

(c) Ge (111)

Fig. 7 Micrographs of the workpiece centers machined at an undeformed chip thickness of 160 nm

removal rate in the ductile machining regime. Figure 8 is a Nomarski micrograph of the workpiece center after machining. Under these conditions, the machined surface was uniform in texture, with no micro-fracture across the entire surface. Figure 9 is a laser probe scanned three-dimensional topography of the finished surface. Although periodical tool-feed marks left by the diamond tool can be clearly seen, no micro-fracture appears. The surface roughness is 58 nm Ry, and 7 nm Ra, respectively.

The above results demonstrate an important fact that the crystallographic anisotropy effect in material

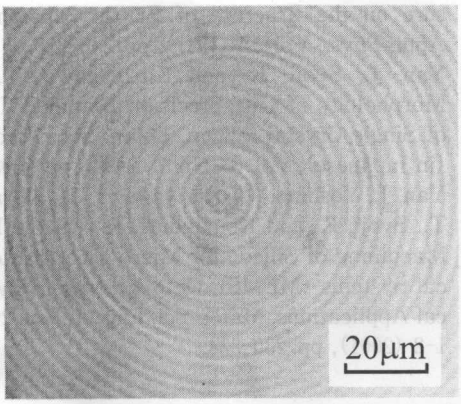

Fig. 8 Micrograph of the workpiece center of Ge (111) at an undeformed chip thickness of 55 nm

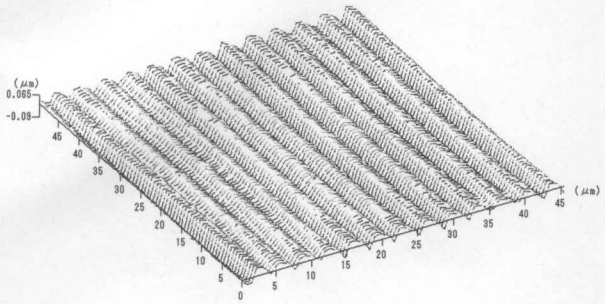

Fig. 9 Three-dimensional topography of the Ge (111) surface machined at an undeformed chip thickness of 55 nm

removal mechanism can be significantly eliminated by decreasing undeformed chip thickness down to the range of a few tens of nanometers, the same level as the tool edge radius. This phenomenon is also considered to originate from the hydrostatic pressure generated in the cutting region, ahead of and beneath the cutting tool, due to the negative effective rake angle caused by the edge radius. Under high hydrostatic pressure, the resolved tensile stresses on the cleavage planes of the crystal will be significantly counteracted and become insufficient to initiate cleavage fracture even for those orientations that are most difficult to be ductile-cut. Therefore, the high pressure phase transformation[3),(4)] and the plastic deformation will dominate the material removal mode despite of the change in crystal orientation. From this aspect, it is indicated that the hydrostatic stress state in the cutting region is essential for the ductile machining process of single-crystal germanium, and that the hydrostatic stress state maybe achieved by optimizing the effective rake angle of the cutting tool.

4. Conclusions

Single-point diamond turning experiments were carried out on single-crystal germanium (100), (110) and (111) planes in an attempt to examine their ultraprecision ductile machinability. Three kinds of surface textures and chip morphologies were generated during the brittle-ductile transition of the machining regimes. Ductile machinability exhibits strong crystallographic anisotropy, leading to micro-fractured surface regions distributing in a radial pattern from the workpiece center. The minimum critical undeformed chip thicknesses for obtaining completely ductile-cut surfaces on all the three crystal planes are approximately the same (60 nm). Below this boundary condition, uniformly ductile-cut surfaces with nanometric roughness can be obtained with yielding plastically-deformed continuous chips. Compared to wet cuts, dry cuts are beneficial for ductile machining on a few specific crystal orientations.

Acknowledgements

This study has been supported by a research grant from the Mitutoyo Association for Science and Technology (MAST), and partially supported by a Grant-in-Aid for Young Scientists (Project Number 15760073) from the Ministry of Education, Science, Sports and Culture of Japan. The authors would like to extend their thanks to Prof. Dr. Katsuo Syoji of Tohoku University for his great supports and valuable discussion.

References

(1) Nakasuji, T., Kodera, S., Hara, S., Matsunaga, H., Ikawa, N. and Shimada, S., Diamond Turning of Brittle Materials for Optical Components, Ann. CIRP, Vol. 39, No. 1 (1990), pp. 89-92.

(2) Blake, P.N. and Scattergood, R.O., Ductile Regime Machining of Germanium and Silicon, J. Amer. Ceram. Soc., Vol. 73, No. 4 (1990), pp. 949-957.

(3) Clarke, D.R., Kroll, M.C., Kirchner, P.D. and Cook, R.F., Amorphization and Conductivity of Silicon and Germanium Induced by Indentation, Phys. Rev. Lett., Vol. 60, No. 21 (1988), pp. 2156-2159.

(4) Morris, J.C., Callahan, D.L., Kulik, J., Patten, J.A. and Scattergood, R.O., Origins of the Ductile Regime in Single-Point Diamond Turning of Semiconductors, J. Am. Ceram. Soc., Vol. 78, No. 8 (1995), pp. 2015-2020.

(5) Yan, J., Syoji, K., Kuriyagawa, T. and Suzuki, H., Ductile Regime Turning at Large Tool Feed, J. Mater. Proc. Tech., Vol. 121 (2002), pp. 363-372.

(6) Yan, J., Syoji, K. and Kuriyagawa, T., Fabrication of Large-Diameter Single-Crystal Silicon Aspheric Lens by Straight-Line Enveloping Diamond-Turning Method, J. Jap. Soc. Prec. Eng., (in Japanese), Vol. 68, No. 4 (2002), pp. 1561-1565.

(7) Yan, J., Syoji, K. and Kuriyagawa, T., Ductile-Brittle Transition under Large Negative Rake Angles, J. Jap. Soc. Prec. Eng., (in Japanese), Vol.

66, No. 7 (2000), pp. 1130-1134.
(8) Yan, J., Syoji, K. and Kuriyagawa, T., Some Aspects on the Optimization of Ductile Regime Cutting Process, Proc. Inter. Conf. on Adv. Manuf. Sys. & Manuf. Auto. (AMSMA), Guangzhou, China, (2000), pp. 185-189.
(9) Johnson, K.L., The Correlation of Indentation Experiments, J. Mech. Phys. Solids, Vol. 18, No. 2 (1970), pp. 115-126.
(10) Johnson, W. and Mellor, P.B., Engineering Plasticity, (1973), Van Nostrand Reinhold Co., London.
(11) Bridgman, P.W., The Effect of Hydrostatic Pressure on the Fracture of Brittle Substances, J. Appl. Phys., Vol. 18 (1947), pp. 246-258.
(12) Yan, J., Syoji, K. and Kuriyagawa, T., Chip Morphology of Ultraprecision Diamond Turning of Single Crystal Silicon, J. Jap. Soc. Prec. Eng., (in Japanese), Vol. 65, No. 7 (1999), pp. 1008-1012.
(13) Yan, J., Yoshino, M., Kuriyagawa, T., Shirakashi, T., Syoji, K. and Komanduri, R., On the Ductile Machining of Silicon for Micro Electro-Mechanical Systems (MEMS), Opto-Electronic and Optical Applications, Mater. Sci. Eng. A, Vol. 297, No. 1-2 (2001), pp. 230-234.